Exact steady-state analysis in multiple-input converters applied with diverse time-sharing switching schemes

Xian, Liang; Wang, Youyi

2015

Xian, L., Wang, Y. (2015). Exact steady-state analysis in multiple-input converters applied with diverse time-sharing switching schemes. IET Power Electronics, 8(5), 724-734.

https://hdl.handle.net/10356/79315

https://doi.org/10.1049/iet-pel.2013.0942

Exact Steady-State Analysis in Multiple-Input Converters Applied with Diverse Time-Sharing Switching Schemes

Journal:	*IET Power Electronics*
Manuscript ID:	PEL-2013-0942.R1
Manuscript Type:	Research Paper
Date Submitted by the Author:	n/a
Complete List of Authors:	Xian, Liang; Nanyang Tecnological University, School of Electrical and Electronics Wang, Youyi; Nanyang Technological University, Division of Power Engineering;
Keyword:	DC-DC POWER CONVERTORS, MULTIPLYING CIRCUITS, TIME DIVISION MULTIPLEXING

IET PEL-2013-0942

Response to the Comments Advised by Reviewer 1

We want to sincerely thank the Editor and the Reviewers for their time and effort in providing valuable and constructive comments. We have considered all the points raised by the Reviewers and are pleased to provide the following response. We have also taken the opportunity to carry out a comprehensive editorial revision of the manuscript so as to improve on the clarity of the article.

Comment 1: In its current state, the level of English through authors' manuscript does not meet the desired standard. There are a number of grammatical errors and instances of badly worded/constructed sentences.

Response:
We realize the high expectation of the IET Power Electronics Journal on the quality/presentation standards of received manuscript and have therefore made every effort to meet this expectation. Accordingly and as pointed out earlier, we have undertaken another round of editorial revision of the article, with the view to correct any grammatical mistakes that may have existed and to improve on the clarity of the article and emphasize our original contributions and research focus. It also benefited from proofreading by native English speakers.

Comment 2: The proposed method leads to higher accuracy when in compared to SSA at the expense of more complexity. How far does it stand for its usefulness?

Response:
We're not going to compare the proposed method with SSA as they have absolutely diverse goals. As was said in the first part of the manuscript, the SSA method aims to provide DC/AC circuit analysis techniques for switching mode power conversion circuits, including their steady-state approximation, dynamic response to variations, stability and robustness analysis, control system design. It's a comprehensive and well-developed tool. But the proposed method in this manuscript is especially aiming to the steady-state analysis to diverse multiple-input converter's topologies and related switching functions. The reason we mentioned SSA in the original manuscript was to try to emphasize that: not like that in conventional SISO conversion circuit, SSA is unable to execute an accurate prediction of the steady-state parametric expressions of the MIC topologies since it cannot track the information that the MIC's specific circuit structures and switching functions bring about. Similar discussion can be found in many literatures, such as [1]. The method in the manuscript takes great care of the information brought by diverse topologies and switching functions and provides high-accurate explicit expressions for system's steady states.

However, as for this comment you put forward to us, we've been reassessing the structural logicality and rationality of the Introduction part and decided to abridge the content about SSA, after all steady-state analysis is not the strength of SSA. We've rearranged the sentences and paragraphs in order to make our motivations and the proposed method's contributions more directly and clearly.

Furthermore, we've changed the title of the manuscript and emphasized "Steady-State Analysis", "Multiple-Input Converters", and "Time-Sharing Switching Schemes" are the three highlights of this manuscript's topic, in order to eliminate the ambiguity/misunderstanding that may cause to readers. Please refer to the Abstract and the Introduction part in the revision manuscript for our efforts.

Besides, we are not noting that equation (1) through (6) are summarized from SSA in order to show that we are not going to make a comparison with our analytical expressions and results to SSA.

We are sincerely appreciated and very ready to hear from your further comments/questions to this manuscript's contribution and novelty at any time, and not hesitating to modify and improve it according to what you are going to recommend.

Comment 3: There are too many abbreviations and parametric reasoning which make reader confused!!!

Response:
We've noticed your suggestion and agreed that it is not necessary to make such a sophisticated nomenclature. We've done the following efforts to make the contents clearer:

(a) To abridge the Nomenclature part in the revision manuscript, only preserving the most-common-used abbreviations, most of which can be found in other published literatures.
(b) List of symbols was removed from the Nomenclature part, just denoting when firstly-mentioned in the contents.
(c) Nomenclature to symbols of parameters used in figures and equations are modified for brevity and better understanding. Symbols, such as V_{ei}, V_{eDi}, d_{ei}, V_{ei1}, etc., were cancelled as well as some with relatively longer or confusing subscripts, such as I_{Linii}, I_{Lfwini}, $I_{Lfwinii}$, etc., were replaced with more brief and generalized counterparts.

Comment 4: Steady-state average method considers the effects of input voltage variations and load changes; how would the presented method include such effects (a new method should be applicable to all conditions).

Response:
As is discussed in the response to the second comment above, the proposed method is the universal exact steady-state analysis tool for a variety of multiple-input converters' topologies which are applied with the specified time-sharing switching functions (TEM and IDEM). It's only focusing on how to find a universal way of expressing the different MIC systems' static operating points (equilibrium points) with known quantities of the parameters explicitly. We're not going to discuss the system's dynamic response or robustness analysis by using this method. We have to admit it's not a modeling method like SSA, but we unconsciously wrongly-define it as a universal model approach in the original manuscript. Your precious comments and questioning reminded us of this overstatement, and we want to express our sincere apology to make you and other reviewers confused.

What we've remedied in our revision manuscript for avoiding ambiguity are as follows:

(a) To modify the title of the original manuscript, avoiding "modeling" but adding "steady-state analysis";
(b) To mend and polish the Abstract and Introduction parts as we specified in the response to Comment 2;
(c) To modify the title of each section/subsection, avoiding "modeling" or "model" word;
(d) To remove all contents about SSA, avoiding comparison with SSA.

Comment 5: Page 7, after equation (8) how do the authors prove from equation (7) that (3) holds in UM in CCM mode using inductor volt second balance?

Response:

As was said in the original manuscript, according to IVSB, equation (3) is an acknowledged expression to reveal the relation between output voltage and input voltages, which was derived by many published literatures in detail [2-5]. Without using IVSB but using the proposed method hereby, such the result can also be obtained from equation (7). In order to clarify our explanation, equation (7) in the original manuscript is rewritten as follows and marked as equation (1):

$$\begin{cases} i_{L1}(t) = I_{Lini1} + (V_1 - V_o)(t - t_0)/L, & t \in [t_o, t_1], \\ i_{L2}(t) = I_{Lini2} + (V_2 - V_o)(t - t_1)/L, & t \in [t_1, t_2], \\ \quad \vdots & \\ i_{Lm}(t) = I_{Linim} + (V_m - V_o)(t - t_{m-1})/L, & t \in [t_{m-1}, t_m], \\ i_{Lfw}(t) = I_{Lfwini} + (-V_o)(t - t_m)/L, & t \in [t_m, t_{m+1}]. \end{cases} \tag{1}$$

If we respectively substitute t_1, t_2, …, t_{m+1} into each sub-equations in (1), we can get the inductor current ripples for every subintervals:

$$\begin{cases} |\Delta i_{L1}(t)| = \dfrac{(V_1 - V_o)d_1}{Lf}, \\ |\Delta i_{L2}(t)| = \dfrac{(V_2 - V_o)d_2}{Lf}, \\ \quad \vdots \\ |\Delta i_{Lm}(t)| = \dfrac{(V_m - V_o)d_m}{Lf}, \\ |\Delta i_{Lfw}(t)| = \dfrac{V_o d_{m+1}}{Lf}. \end{cases} \tag{2}$$

From Fig. 3(a), we can see that the sum of the first m sub-equations in (2) equals to the (m+1)th sub-equation in (2), as such:

$$\begin{aligned} &\textstyle\sum_1^m |\Delta i_{Li}(t)| = \dfrac{\sum_1^m (V_i - V_o)d_i}{Lf} = |\Delta i_{Lfw}(t)| = \dfrac{V_o d_{m+1}}{Lf}, \\ &\Rightarrow \textstyle\sum_1^m V_i d_i - V_o \sum_1^m d_i = V_o d_{m+1}, \\ &\Rightarrow V_o \textstyle\sum_1^{m+1} d_i = \sum_1^m V_i d_i, \\ &\Rightarrow V_o = \textstyle\sum_1^m V_i d_i, \end{aligned} \tag{3}$$

the final derivation result of which is exactly the same as that in equation (3) in the original manuscript. Proven!

In order to prevent misunderstanding for readers, we modified the related description sentences as "Equation (3) in CCM is derived from the inductor volt-second balance principle [4, 7, 10, 16], and identical result can be easily derived from (7) as well.", which was yellow-highlighted in the revision manuscript.

Comment 6: As the authors mention in section III, IDEM-based TSS technique cannot be applied to MIbC topology in DCM. Isn't it a weakness!!!

Response:

As was noted in the first paragraph of Section III in the original manuscript, the reason we are not talking about the DCM scenario is that the IDEM DCM is an abnormal case which is highly discouraged in practical applications. According to our knowledge, no published literature has ever discussed on this situation, even the IDEM CCM instances are numbered. If there are m inputs in the MIC circuit, the DCM case will cause m local-extreme-point-to-zero current variations plus another m zero-to-next-local-extreme-point variations flowing through the common inductor L, which can be deemed as a high-frequent pulsating current source with the switching frequency m times higher than the fundamental frequency of the applied switching functions, f. The following illustration, Fig. 1, about this DCM case is presented for better understanding. Such operation mode has extremely negative effect on components and system's stability and reliability, and will escalate as the number of inputs increases. The load terminal will also suffer this high-frequent discontinuous current source, which is very awful and not practical especially the load is the DC/AC power grid.

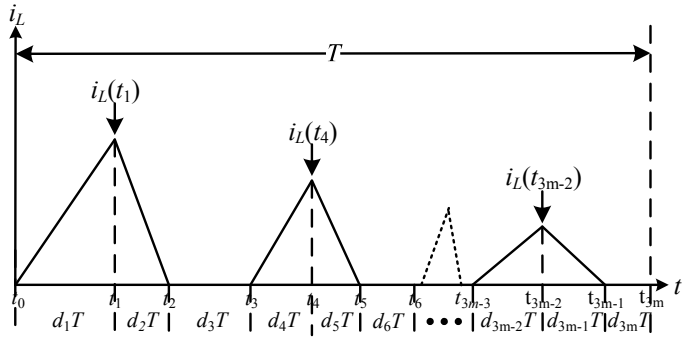

Fig. 1. Waveforms of i_L dynamic in m-input MIbC responding to IDEM TSS strategy in DCM.

Not being given this impractical scenario a specific steady-state analysis in this manuscript, though, doesn't mean our proposed method cannot be applied to this scenario. This steady-state analysis and expression derivation method is universally suitable for all types of MIC circuits, however, due to the page limitation, it is impossible for us to provide details with every one of them. The questioning and suggestion you put forward in this comment and the next comment are very crucial for us to rethink about this section's structure. In order to make the series of the analytical expressions for MICs more comprehensive and generalized for readers, we rebuilt the organization of Section II and III and added two new subsections talking about output voltage ripple issues and universal procedure to do the analysis and derivation to other types of MIC in the new Section III. Appendix is also provided to list out the derivative results when the proposed method is utilized in another two popular MIC topologies: multiple-input buck-boost converter (MIbBC) [3, 6-16] and multiple-input single-ended

primary-inductor converter (MISEPIC)[1, 17-19], by using the very procedure presented in Section III-A.

Aiming to the question in this comment, though we made the final decision after cautious discussion that not involving the IDEM DCM case in this manuscript for the reason we above-mentioned, we are willing to made more effort here on this scenario, not only for answering the question you put forward, but also for making ourselves more confident and clearer that our proposed method is definitely a universal steady-state analytical tool for MICs with diverse switching functions operating in CCM/DCM. Thus, here come the details.

According to Fig. 1, the inductor current profile has the following piece-wise expression:

$$i_L(t)=\begin{cases}\begin{cases}(V_1-V_o)(t-t_0)/L, & t\in[t_o,t_1]\\ i_L(t_1)+(-V_o)(t-t_1)/L, & t\in[t_1,t_2]\\ 0\cdot(t-t_2) & t\in[t_2,t_3]\end{cases}\\ \begin{cases}(V_2-V_o)(t-t_3)/L, & t\in[t_3,t_4]\\ i_L(t_4)+(-V_o)(t-t_4)/L, & t\in[t_4,t_5]\\ 0\cdot(t-t_5) & t\in[t_5,t_6]\end{cases}\\ \quad\vdots\\ \begin{cases}(V_m-V_o)(t-t_{3m-3})/L, & t\in[t_{3m-3},t_{3m-2}]\\ i_L(t_{3m-2})+(-V_o)(t-t_{3m-2})/L, & t\in[t_{3m-2},t_{3m-1}]\\ 0\cdot(t-t_{3m-1}). & t\in[t_{3m-1},t_{3m}]\end{cases}\end{cases} \tag{4}$$

The terms, $i_L(t_1)$, $i_L(t_2)$, …, $i_{Lm}(t_{3m-2})$, can be specified with their upper equations. With similar equating and iteration process to CCM case, (4) is optimized to the following expression set:

$$i_L(t)=\begin{cases}\begin{cases}(V_1-V_o)(t-t_0)/L, & t\in[t_o,t_1]\\ (V_1-V_o)d_1/Lf-(t-t_1)V_o/L, & t\in[t_1,t_2]\\ 0\cdot(t-t_2) & t\in[t_2,t_3]\end{cases}\\ \begin{cases}(V_2-V_o)(t-t_3)/L, & t\in[t_3,t_4]\\ (V_2-V_o)d_4/Lf-(t-t_4)V_o/L, & t\in[t_4,t_5]\\ 0\cdot(t-t_5) & t\in[t_5,t_6]\end{cases}\\ \quad\vdots\\ \begin{cases}(V_m-V_o)(t-t_{3m-3})/L, & t\in[t_{3m-3},t_{3m-2}]\\ (V_m-V_o)d_{3m-2}/Lf-(t-t_{3m-2})V_o/L, & t\in[t_{3m-2},t_{3m-1}]\\ 0\cdot(t-t_{3m-1}). & t\in[t_{3m-1},t_{3m}]\end{cases}\end{cases} \tag{5}$$

It is a (3 x m)-equation set which can be rearranged into m subintervals as (5) shows. It is an equivalent to m independent conventional single-input single-output (SISO) buck converters consecutively conducted in DCM during one original operating period, T. Here in (5) the implicit elements are the nonzero freewheeling durations, i.e., d_2T, d_5T, …, $d_{3m-1}T$, plus the output voltage, V_o, itself. It can be optimized to the following expression set:

$$i_L(t)=\begin{cases}(V_i-V_o)(t-t_{i-1})/L, & t\in[t_{3i-3},t_{3i-2}]\\ (V_i-V_o)d_{3i-2}/Lf-(t-t_{3i-2})V_o/L, & t\in[t_{3i-2},t_{3i-1}]\\ 0\cdot(t-t_{3i-1}). & t\in[t_{3i-1},t_{3i}]\end{cases}\quad i=1,2,\cdots,m \tag{6}$$

Similar to the derivation process as in (19) of the original manuscript, the averaged inductor current for

each subinterval:

$$I_L(t) = (V_i - V_o)d_{3i-2}^2 / (2Lf) + (V_i - V_o)d_{3i-2}d_{3i-1} / Lf - d_{3i-1}^2 V_o / (2Lf), \quad t \in [t_{3i-3}, t_{3i}]. \tag{7}$$

According to [10], the implicit elements d_2, d_5, …, d_{3m-1} can be solved by using the following equation:

$$d_{3i-1} = (V_i - V_o)\, d_{3i-2} / (fV_o). \tag{8}$$

Derived from the energy balance theory, the following nonlinear equation should be solved numerically to obtain the output voltage:

$$\frac{\sum_1^m (V_i - V_o)^2 d_{3i-2}^2}{2Lf^2} = \frac{V_o^2}{R}\left(m - \sum_1^m d_{3i-2}\right). \tag{9}$$

With the help of (7) through (9), the explicit expression for I_L can be readily solved as:

$$I_L(t) = \sum_1^m \left[(V_i - V_o)d_{3i-2}^2 / (2Lf) + (V_i - V_o)d_{3i-2}d_{3i-1} / Lf - d_{3i-1}^2 V_o / (2Lf)\right]. \tag{10}$$

It is easy to see from (10) that the average inductor current is no more than the sum of average values for m subintervals that divided in (5). Each of them can be deemed as an independent SISO buck converter. The IDEM-based DIbC in DCM is just a case of algebraic sum of m SISO buck converters with m different inputs within one operating period, T. Till now all the general formulas for IDEM-based DIbC in DCM are derived explicitly.

Comment 7: A new theory should be generalized for all converters!!!! Applying it only to a MIC doesn't verify it. It needs to be tested in different MICs with variety of switching functions.

Response:
As is provided in the response to Comment 6, we did the following improvement in our revision manuscript to make the method more convincible in its generality:

(a) To add a new subsection talking about the proposed method for the output voltage ripple issues in Section III-B;
(b) To provide universal procedures to do steady-state analysis and derivation for all types of MIC circuits in the newly-added Section III-A;
(c) To give a list about the derived analytical expressions (general form of equations) for the MIbBC and MISEPIC topologies in the newly-added Appendix part.
(d) To add detailed analysis for IDEM DCM case in Section II-B (not adopted because of page limitation and impracticality).

Comment 8: How this theory can be used for circuit design, same as SSA method? It is not discuss here.

Response:
The derivation of GFEs and their experimental verification and comparison let us better understand the operating behaviors of all the crucial circuit's parameters in MIC. The dynamics of the circuit's parameters under different TSS schemes show obvious disparities, which is very important when we are designing a MIC circuit. According to these conclusions and GFEs, components parameters in MIC

circuit, such as boundary common inductor L_b, total inductor current ripple over one operating period $|\Delta i_L|$, on-resistances of switches, ESR of L, can be accurately calculated. The choice of modulation type, arrangement of input voltages, and boundaries of duty ratios and frequency in the circuit design can be determined more reasonably. Some related description was added to the Conclusion part. We only present the conclusions that we found in the experiments of this study, and according to these conclusions researchers can benefit from variety of issues in the circuit design. However, due to page limitation and less correlation to the research scope of this manuscript, we are unable to discuss them one by one, just briefly mentioning in Section IV and the Conclusion part.

Comment 9: As it is listed in table 1, how does new theory discuss input voltage and output voltage variations? It doesn't discuss dynamic response to input voltage and output voltage variations?

Response:

As is discussed in the response to the second comment above, the proposed method is the universal exact steady-state analysis tool for a variety of multiple-input converters' topologies which are applied with the specified time-sharing switching functions (TEM and IDEM). It's only focusing on how to find a universal way of expressing the different MIC systems' static operating points (equilibrium points) with known quantities of the parameters explicitly. We're not going to discuss the system's dynamic response or robustness analysis by using this method. We have to admit it's not a modeling method like SSA, but we unconsciously wrongly-define it as a universal model approach in the original manuscript. Your precious comments and questioning reminded us of this overstatement, and we want to express our sincere apology to make you and other reviewers confused. What we've paid great effort in our revision manuscript for answering your questioning of this comment are as follows:

(a) To modify the title of the original manuscript, avoiding "modeling" but adding "steady-state analysis";
(b) To modify the Abstract and Introduction parts as we specified in the response to Comment 2;
(c) To modify the title of each section/subsection, avoiding "modeling" or "model" word;
(d) To combined the original Section II and III into one, Section II, and add a new section after that to talk about the scenario of the output voltage ripple of MIC. In the newly-added Section III, a universal procedure to do the analysis and expression derivation is presented, in order to make the series of the analytical expressions for MICs more comprehensive and generalized.

We are sincerely appreciated and very ready to hear from your further response and perspective to what we did for this comment, and not hesitating to rewrite/enhance our manuscript if necessary at any time.

Reference

[1] Z. Ruichen, Y. Sheng-Yang, and A. Kwasinski, "Modeling of multiple-input DC-DC converters considering input-coupling effects," in *Energy Conversion Congress and Exposition (ECCE), 2011 IEEE*, 2011, pp. 698-705.

[2] H. Behjati, L. Niu, A. Davoudi, and P. L. Chapman, "Alternative Time-Invariant Multi-Frequency Modeling of PWM DC-DC Converters," *Ieee Transactions on Circuits and Systems I-Regular Papers,* vol. 60, pp. 3069-3079, Nov 2013.

[3] K. Gummi and M. Ferdowsi, "Double-Input DC-DC Power Electronic Converters for Electric-Drive Vehicles-Topology Exploration and Synthesis Using a Single-Pole Triple-Throw Switch," *Industrial Electronics, IEEE Transactions on,* vol. 57, pp. 617-623, 2010.

[4] A. Kwasinski and P. T. Krein, "Multiple-input dc-dc converters to enhance local availability in grids using distributed generation resources," in *Applied Power Electronics Conference, APEC 2007 - Twenty Second Annual IEEE*, 2007, pp. 1657-1663.

[5] Y. Dongsheng, Y. Min, and R. Xinbo, "One-Cycle Control for a Double-Input DC/DC Converter," *Power Electronics, IEEE Transactions on,* vol. 27, pp. 4646-4655, 2012.

[6] L. Yan, R. Xinbo, Y. Dongsheng, and L. Fuxin, "Modeling, analysis and design for hybrid power systems with dual-input DC/DC converter," in *Energy Conversion Congress and Exposition, 2009. ECCE 2009. IEEE*, 2009, pp. 3203-3210.

[7] C. N. Onwuchekwa and A. Kwasinski, "Analysis of boundary control for a multiple-input DC-DC converter topology," in *Applied Power Electronics Conference and Exposition (APEC), 2011 Twenty-Sixth Annual IEEE*, 2011, pp. 1232-1237.

[8] G. Y. Ding and A. Kwasinski, "Digital constant on-time controlled Multiple-input buck and buck-boost converters," *2013 Twenty-Eighth Annual Ieee Applied Power Electronics Conference and Exposition (Apec 2013),* pp. 1376-1382, 2013.

[9] C. N. Onwuchekwa and A. Kwasinski, "A Modified-Time-Sharing Switching Technique for Multiple-Input DC-DC Converters," *Power Electronics, IEEE Transactions on,* vol. 27, pp. 4492-4502, 2012.

[10] C. Yongxiang, A. Davoudi, and P. L. Chapman, "Multifrequency modeling of a multiple-input Dc-Dc converter," in *Power Electronics Specialists Conference, 2008. PESC 2008. IEEE*, 2008, pp. 4604-4610.

[11] A. Khaligh, J. Cao, and Y. J. Lee, "A Multiple-Input DC-DC Converter Topology," *Ieee Transactions on Power Electronics,* vol. 24, pp. 862-868, Mar-Apr 2009.

[12] H. Behjati and A. Davoudi, "A Multiple-Input Multiple-Output DC-DC Converter," *Industry Applications, IEEE Transactions on,* vol. 49, pp. 1464-1479, 2013.

[13] R. Ahmadi, H. Zargarzadeh, and M. Ferdowsi, "Nonlinear Power Sharing Controller for a Double-Input H-Bridge-Based Buckboost-Buckboost Converter," *Power Electronics, IEEE Transactions on,* vol. 28, pp. 2402-2414, 2013.

[14] N. D. Benavides and P. L. Chapman, "Power budgeting of a multiple-input buck-boost converter," *Power Electronics, IEEE Transactions on,* vol. 20, pp. 1303-1309, 2005.

[15] D. Somayajula and M. Ferdowsi, "Power Sharing in a Double-Input Buckboost Converter Using Offset Time Control," in *Applied Power Electronics Conference and Exposition, 2009. APEC 2009. Twenty-Fourth Annual IEEE*, 2009, pp. 1091-1096.

[16] N. D. Benavides, T. Esram, and P. L. Chapman, "Ripple Correlation Control of a Multiple-Input Dc-Dc Converter," in *Power Electronics Specialists Conference, 2005. PESC '05. IEEE 36th*, 2005, pp. 160-164.

[17] D. Somayajula and M. Ferdowsi, "Small-signal modeling and analysis of the double-input buckboost converter," in *Applied Power Electronics Conference and Exposition (APEC), 2010 Twenty-Fifth Annual IEEE*, 2010, pp. 2111-2115.

[18] Z. Ruichen and A. Kwasinski, "Analysis of decentralized controller for multiple-input converters," in *Applied Power Electronics Conference and Exposition (APEC), 2012 Twenty-Seventh Annual IEEE*, 2012, pp. 1853-1860.

[19] S. Junseok and A. Kwasinski, "Analysis of the effects of duty cycle constraints in multiple-input converters for photovoltaic applications," in *Telecommunications Energy Conference, 2009. INTELEC 2009. 31st International*, 2009, pp. 1-5.

[20] Z. Ruichen and A. Kwasinski, "Multiple-input single ended primary inductor converter (SEPIC) converter for

distributed generation applications," in *Energy Conversion Congress and Exposition, 2009. ECCE 2009. IEEE*, 2009, pp. 1847-1854.

IET PEL-2013-0942

Response to the Comments Advised by Reviewer 2

We want to sincerely thank the Editor and the Reviewers for their time and effort in providing valuable and constructive comments. We have considered all the points raised by the Reviewers and are pleased to provide the following response. We have also taken the opportunity to carry out a comprehensive editorial revision of the manuscript so as to improve on the clarity of the article.

Comment 1: The paper needs to be shortened.

Response:
We realize the high expectation of the IET Power Electronics Journal on the quality/presentation standards of received manuscript and have therefore made every effort to meet this expectation. This manuscript proposes an exact steady-state analysis tool specific for all MIC topologies applied with diverse switching functions and operating in CCM/DCM. A detailed derivation course is firstly needed to show the method's origin and operational principles. Because it is a general analytical method, every possible scenario is needed to discussed, here we have three scenarios as that in Section II which take a large amount of contents. Then a general procedures for derivation benefiting to other types of MIC topologies are summarized in Section III-A, which is also significant for the completeness and generality of this method. After that, experiments results and comparison discussion are included for verification the accuracy and feasibility of the method. Finally, for convenience of researchers' further study, general form of equations derivation results should be listed as an Appendix. However, we noticed your recommendation and did every effort we could to make the manuscript more integrated and simplified to readers:

(a) To simplify the Nomenclature part, abridging Abbreviation words by keeping some common-used ones and removing others, removing Symbols part by giving the notation in the contents.
(b) We give up using matrix form to express equations and replacing with general form of equations instead in order to make the contents clearer and more precisely.
(c) We regulate the structure of the contents, combining the original Section II and III into one and added the new Section III with generalization procedures that could be used to handle with the issues of any other MIC topology.
(d) Equations derivation results for another two MIC topologies are concluded in the newly-added Appendix part.
(e) Tables and figures in experiments are shortened, removing unnecessary description and data.

We are sincerely appreciated and very ready to hear from your further comments/questions to this manuscript's contribution and novelty at any time, and not hesitating to modify and improve it according to what you are going to recommend.

IET PEL-2013-0942

Response to the Comments Advised by Reviewer 3

We want to sincerely thank the Editor and the Reviewers for their time and effort in providing valuable and constructive comments. We have considered all the points raised by the Reviewers and are pleased to provide the following response. We have also taken the opportunity to carry out a comprehensive editorial revision of the manuscript so as to improve on the clarity of the article. We are sincerely appreciated and very ready to hear from your further comments/questions to this manuscript's contribution and novelty at any time, and not hesitating to modify and improve it according to what you are going to recommend.

Exact Steady-State Analysis in Multiple-Input Converters Applied with Diverse Time-Sharing Switching Schemes

***Abstract*—Time-sharing switching (TSS) techniques are usually utilized in multiple-input converters (MICs) to manage power sharing among inputs as well as output-voltage regulation. The two most-commonly-used TSS schemes in practical MIC applications are trailing-edge modulation (TEM) and interleaved dual-edge modulation (IDEM), both of which containing abundant significant information on conduction sequence. Steady-state analysis and computation help understand MICs' behavior, being of high significance in both principal and practical researches. The study exhibits a general and exact methodology for computing and synthesizing analytical expressions in steady state of any kind of MIC topology, based upon analysis of segmented waveforms of common inductor current and output capacitor voltage. The derivation results are of high accuracy and generality, applicable for scenarios with arbitrary number of inputs in either continuous conduction mode or discontinuous conduction mode, and applied by either TEM-based or IDEM-based TSS schemes. Analytical and derivation details are addressed to the issues of multiple-input buck converters, along with general procedures established for other MIC's topologies, e.g. multiple-input buck-boost converters and multiple-input single-ended primary-inductor converters. Case study on a dual-input buck converter prototype, considering power dissipations and voltage drops on its components, is put forward for theoretical verification.**

***Index Terms*—DC-DC power converter, multiport circuits, steady-state analysis, continuous conduction mode, discontinuous conduction mode, time division multiplexing**

NOMENCLATURE

Abbreviation

SISO	single-input single-output
MIC(s)	multiple-input converter(s)
MIbC(s)	multiple-input buck converter(s)
PWM	pulse-width modulation
TSS	time-sharing switching
TEM	trailing-edge modulation
IDEM	interleaved duel-edge modulation
DIbC(s)	double-input (or duel-input) buck converter(s)

Comment [#L1]: The title of the manuscript is modified, emphasizing "Steady-State Analysis", "Multiple-Input Converters", and "Time-Sharing Switching Schemes" which are the three highlights of this manuscript's topic, in order to eliminate the ambiguity/misunderstanding that may cause to readers.

Comment [#L2]: Abstract is polished and improved.

Comment [#L3]: Nomenclature is shortened, cancelling the Symbols part and abridging the Abbreviation part. Only those abbreviations appearing frequently in other published literatres are inherited in here in order to avoid ambiguity or misunderstanding.

MIbBC(s)	multiple-input buck-boost converter(s)
CCM	continuous conduction mode
DCM	discontinuous conduction mode
GFE(s)	general form of equation(s)
FCBB	forward-conducting and bidirectional-blocking
MISEPIC(s)	multiple-input single-ended primary-inductor converter(s)

I. INTRODUCTION

Attracting immense attention in renewable-energy-source applications and topology economization, power conversion devices for multiple input sources, in recent decades, are no longer limited to parallel/series-connected several single-input single-output (SISO) converters to bus terminal of output. Characterized with more integrated topology, simpler manipulation, less component count, and comparative higher efficiency, multiple-input converters (MICs) become an attractive candidate for developing multisource hybrid power supply in renewable energy applications [1]. With proper design, the MIC-based circuitry helps improve the availability and the feasibility of those hybrid power supply systems that are able to make rational utilization of diverse sources [2]. One of the most-commonly-used topologies in the MIC family is multiple-input buck (step-down) converter (MIbC) with m-inputs and 1-output, whose fundenmental schematic is presented in Fig. 1(a). As one of the pulse-width modulated (PWM) dc-dc converters, MIC, essentially, belongs to the class of variable-structure time-varying switching systems, whose operating principle and dynamic behavior are based on its applied switching functions. As one of the reliable tools and methodologies to understand the MIC's behavior, the analysis and the computation of steady-state is of great interest for both the theory of electrical network and the extended range of applications.

Time-sharing switching (TSS) technique (or called time division multiplexing scheme) is usually applied to structuring MIC's particular PWM switching functions. In general, it allows more than one switches to operate within one switching operating period, T, on the premise that only one of them should conduct at a given instant. The classification of TSS functions illustrated in Fig. 2 almost covers all the MIC-related literatures: 1) synchronously-triggered trailing-edge modulation (TEM), 2) asynchronously-triggered TEM, and 3) interleaved dual-edge modulation (IDEM). As indicated in Fig. 2(a), the switching patterns of synchronously-triggered TEM on q_1 to q_m conduct simultaneously at the beginning of each T. The operating principle and related applications can be found in [3-5]. Only those inputs strictly arranged in voltage-descending order, (assuring the input with the highest voltage is able to clamp other lower ones and power the load individually), are applicable for synchronous-triggered TEM. Source with neither disordered-voltage nor equal-terminal-voltage is applicable for this technique. In order to overcome this obstacle, the improved strategy, called asynchronous-triggered TEM, was proposed as is illustrated in Fig. 2(b) [6-10]. The conduction periods of all switching patterns are separated while conduction consecutiveness and sequence are retained from the

Comment [#L4]: This paragraph mainly are introducing the origins and principles of the three TSS techniques that are most-commonly-used in MIC circuits. Their applications and research state quo are reviewed. Along with that, the presented typical topologies and switching patterns are of great significance in the analysis and derivation in the following sections.

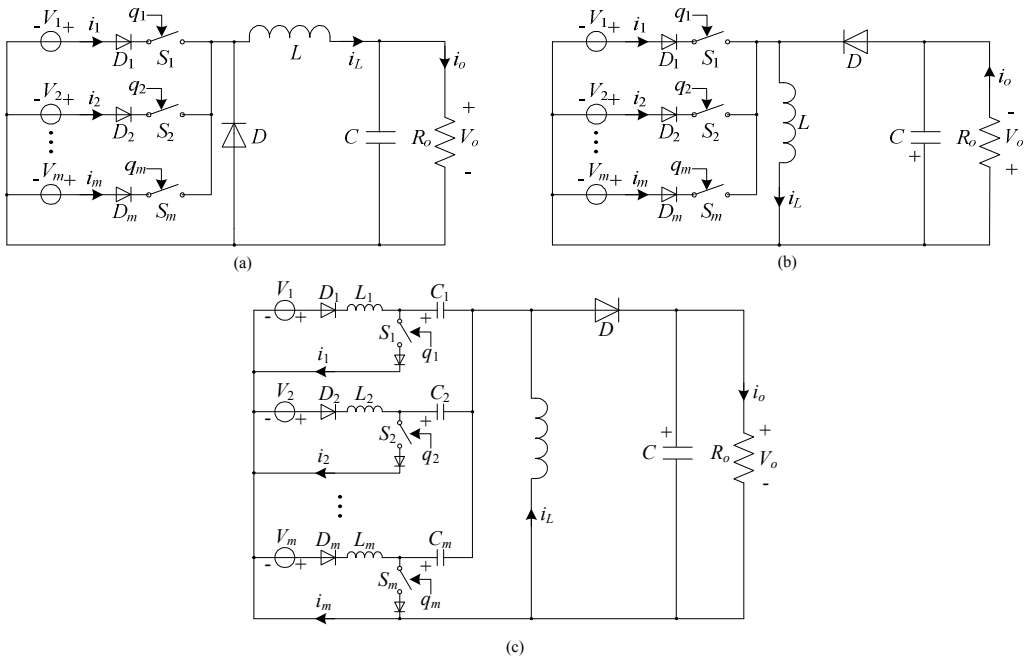

Fig. 1. Typical non-isolated *m*-input topologies of (a) MIbC, (b) MIbBC, and (c) MISEPIC.

Comment [#L5]: Two more typical MIC topologies are added here in (b) and (c), referred by the generalization procedures in Section III-A, to calculate the GFEs for all concerned system's parameters in both TEM and IDEM scenarios as that in MIbC discussed in Section II. They are listed in Appendix. It proves the completeness and feasibility of the proposed analytical and derivation methodology.

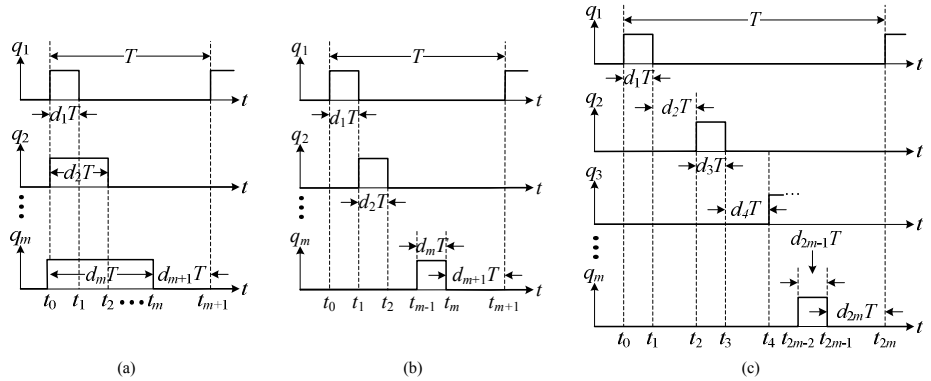

Fig. 2. Universal switching functions/patterns for *m*-input MICs with TSS strategy based on: (a) synchronously-triggered TEM, (b) asynchronously-triggered TEM, and (c) IDEM.

synchronous-triggered one. It is applicable for both voltage-disordered and voltage-equal inputs while sharing the identical effective duty ratios to the synchronously-triggered one, due to which it was hereby applied as the representative of the TEM TSS technique for the analysis and computation hereinafter. Beyond that, IDEM TSS scheme is proven to possess ripple rejection capability in the inductor current of a double-input (or dual-input) buck converter (DIbC) topology [11]. It has already cut a figure not only in some practical dual-input converter control approaches but also to some extended MIC (more than two inputs) issues.

Among them, reference [12] provided us a control approach to power sharing between the two inputs of a DIbC, which was derived from the dead-time effects of the switching functions. The definition of the dead-time, referring to the phase shifts between the two switching functions, actually helped to form a specific case of IDEM. The mathematical derivation therein revealed some forward-looking relations among parameters of the common inductor current. Applied in DIbC as well, reference [13] established an output-voltage regulator via several amplifier circuits and logic-gates to obtain a pair of switching functions with time-varying phase shifts between both. It was certainly another eligible IDEM case, but unfortunately paid little attention to the state-space modeling itself. Besides that, through recombination of logic-gates and toggle flip-flops, modified-TSS technique proposed in [2] which divided one common switching function into arbitrary positive-integral number of interleaved equal-phase-shifted sub-switching functions that respectively served to switches in a multiple-input buck-boost converter (MIbBC); it reduced the topology to a SISO equivalent, and simplified circuit modeling and controller design. It was a successful instance of extending IDEM-based TSS technique to MIC applications, though only some targeted modeling equations were given. Some other analogous applications could be found in [14, 15]. The most-generally-applicable switching patterns as drawn in Fig. 2(c) are applied to represent the IDEM TSS technique, with which all the IDEM TSS strategies used in the aforementioned literatures can be elucidated. For instance, switching functions generated in [2] are equivalent to equating duty ratios $d_1 = d_3 = \ldots = d_{2m-1}$ and $d_2 = d_4 = \ldots = d_{2m}$.

Apparently, TSS scheme involves abundant significant information on conduction sequence and phase shifts, with which MIC should be at a certain number of different modes depending on the possible combinations of the actual state of the. Every scheme provided in Fig. 2 actually consists of $(m + 1)$ combinations and divides one complete operating period into several subintervals. The characteristics of the switching functions yield time dependent coefficients within a set of equations that describe the system's steady state. Among these diverse subintervals, circuit configurations vary periodically and discontinuously, of which should be taken care separately when making the steady-state analysis. Recently, some efforts have been made to exploring such topics but lacking in generality and normalization [1, 16, 17]. This paper therefore aims 1) to explore and reveal exact and universal explicit analytical expressions and parametric relations for MIbC topology with arbitrary number of inputs (m-input) in both continuous conduction mode (CCM) and discontinuous conduction mode (DCM) and applied by both TEM-based and IDEM-based TSS schemes; 2) to provide a systematic steady-state analysis methodology applicable for handling with all types of topologies in non-isolated MIC family.

Comment [#L6]: The motivation and contribution in this manuscript are modified and addressed here.

Due to page limitation, MIbC is used to serve as an illustrative example because of its straightforward circuit configuration and high-frequent appearance in MIC applications [1, 5, 7-9, 13]. The contents of the paper are organized as follows: exact steady-state analysis and derivation in MIbC, based on TEM and IDEM TSS functions and operating in CCM and DCM, will be respectively discussed in Section II; followed by the proposed generalization procedures in Section III, series of analytical expressions for rest

of the MIC topologies besides MIbC could be established (two favored will be listed in Appendix); a MIbC prototype with two input legs will be implemented and studied for theoretical verification in Section IV; finally, conclusions will be drawn.

II. Exact Steady-State Analysis in Multiple-Input Buck Converters

First of all, some clarifications in this study should be hereby put forward:

(a) Mathematically, the objective of Section II is to yield all common-inductor-current-related exact and universal explicit analytical expressions which include and only include all/some of known quantities in MIbC. Those qualified equations in the derivation are hereinafter called the general form of equation (GFE). The known quantities are identified in Table I, considering operational diversity, where f is operating frequency (unit: Hz), L is common inductor and its inductance (unit: H), C is output capacitor and its capacitance (unit: F), R_o is resistive load and its resistance (unit: Ω), V_1-V_m represent m input sources and their voltages (unit: V).

(b) Voltages of V_1, V_2, …, V_m are invariants higher than output voltage and arranged in voltage-descending order. Radom arrangement is considered a special case which will be discussed in Section III.

(c) C is sufficiently large to assume a constant output voltage.

(d) The MIC topologies we discuss here are all unidirectional thus reverse power flow from the load terminal to the inputs should be strictly forbidden. Such one-way power flowing condition is guaranteed by forward-conducting and bidirectional-blocking (FCBB) switches. If the switches in Fig. 1(a) are MOSFETs with reverse parasitic diodes, diodes D_1 to D_m are employed to construct FCBB switches. It should be noted that the diode connecting to the input with highest voltage can be removed.

A. CCM Scenario with TEM-based TSS Scheme

If a synchronous-triggered TEM-based TSS technique as shown in Fig. 2(b) is applied to serve as switching functions for MIbC topology given in Fig. 1, the waveform of i_L should respond like Fig. 3(a) demonstrates, where the entire waveform in one complete operating period is divided into (m + 1) subintervals. The last subinterval, $d_{m+1}T$ is the freewheeling period whose value is determined by the previous m subintervals (i.e., $d_{m+1}=1-\sum_1^m d_i$).

According to Fig. 3(a), the inductor current profile has the following given piecewise linear shape with respect to t (assuming f is much larger than its dynamics),

$$i_L(t)=\begin{cases} i_L(t_0)+(V_1-V_o)(t-t_0)/L & t\in[t_o,t_1] \\ i_L(t_1)+(V_2-V_o)(t-t_1)/L & t\in[t_1,t_2] \\ \quad\vdots & \quad\vdots \\ i_L(t_{m-1})+(V_m-V_o)(t-t_{m-1})/L & t\in[t_{m-1},t_m] \\ i_L(t_m)-V_o(t-t_m)/L & t\in[t_m,t_{m+1}] \end{cases} \quad (1)$$

Comment [#L7]: Symbols in Nomenclature is cancelled, firstly-mentioned symbols are clarified in the contents they located, making the Nomenclature shorter.

Comment [#L8]: The description of all the equations in this manuscript are changed to the general form instead of the matrix form.

TABLE I KNOWN QUANTITIES IN MIBC FOR DIVERSE OPERATIONAL SCENARIOS

Scenario	CCM-TEM	DCM-TEM	CCM-IDEM
Known quantities	T, f, m, L, C, R_o, V_1-V_m, d_1-d_{m+1}	T, f, m, L, C, R_o, V_1-V_m, d_1-d_m	T, f, m, L, C, R_o, V_1-V_m, d_1-d_{2m}

Comment [#L9]: Known quantities, which are needed to expressed all derivation results of GFEs in all scenarios that are going to be discussed below, are listed here for better checking and utilization.

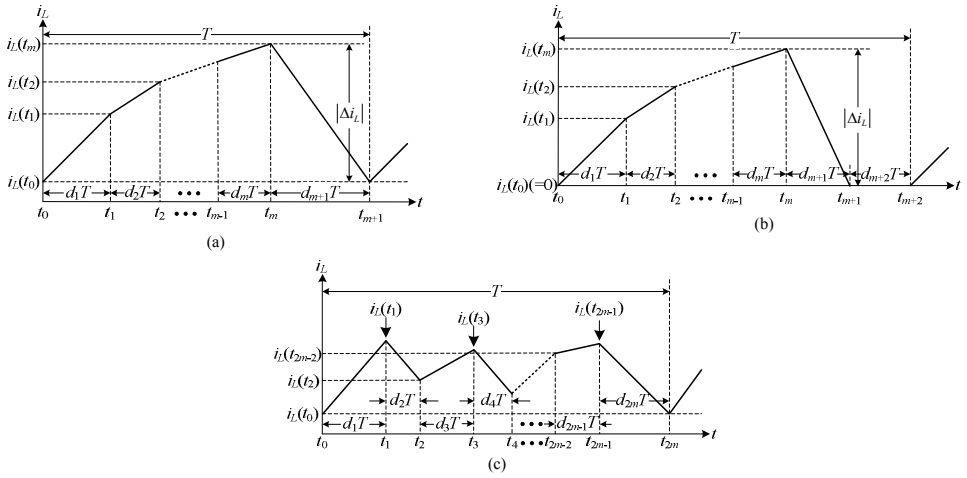

Fig. 3. Waveforms of i_L dynamic in m-input MIbC responding to asynchronously-triggered TEM-based TSS scheme (a) in CCM, (b) in DCM, and (c) IDEM-based TSS scheme (c) in CCM.

The GFE of (1) can be written as

$$i_L(t) = i_L(t_{i-1}) + \frac{(V_i - V_o)(t - t_{i-1})}{L} \qquad t \in [t_{i-1}, t_i] \tag{2}$$

where $i = 1, 2, \ldots, m+1$ and $V_{m+1} = 0$. Respectively substituting $t_1, t_2, \ldots, t_{m+1}$ into the sub-equations in (1) yields the GFE for the ith-subinterval inductor current ripple,

$$|\Delta i_{Li}| = \frac{|V_i - V_o| d_i}{Lf} \qquad t \in [t_{i-1}, t_i] \tag{3}$$

Waveform in Fig. 3(a) indicates that the sum of the first m sub-equations in (1) equals to the $(m+1)$th sub-equation, hence the total inductor current ripple over one operating period is

$$|\Delta i_L| = \frac{|V_i - V_o| \sum_1^m d_i}{Lf} \text{ or } = \frac{V_o d_{m+1}}{Lf} \tag{4}$$

from which we can easily obtain input-to-output GFE

$$V_o = \sum_1^m V_i d_i \tag{5}$$

The identical relation to (5) between inputs and output is also available from the inductor volt-second balance principle [1, 5, 8, 17, 18]. Due to the principle of iterative algorithm, the terms $i_L(t_1)$ to $i_L(t_{m+1})$ in (1) can be replaced with their upper sub-equations, finally uniformly expressed with the initial value, $i_L(t_0)$,

$$i_L(t)=\begin{cases} i_L(t_0)+(V_1-V_o)(t-t_0)/L & t\in[t_o,t_1] \\ i_L(t_0)+(V_1-V_o)d_1/(Lf)+(V_2-V_o)(t-t_1)/L & t\in[t_1,t_2] \\ i_L(t_0)+(V_1-V_o)d_1/(Lf)+(V_2-V_o)d_2/(Lf)+(V_3-V_o)(t-t_2)/L & t\in[t_2,t_3] \\ \quad\vdots & \quad\vdots \\ i_L(t_0)+\sum_1^{m-1}(V_i-V_o)d_i/(Lf)+(V_m-V_o)(t-t_{m-1})/L & t\in[t_{m-1},t_m] \\ i_L(t_0)+\sum_1^{m}(V_i-V_o)d_i/(Lf)-V_o(t-t_m)/L & t\in[t_m,t_{m+1}] \end{cases} \tag{6}$$

Normalize (6) to the GFE for the *i*th-subinterval time-dependent inductor current as

$$i_L(t)=i_L(t_0)+\frac{\sum_1^{i-1}(V_j-V_o)d_j}{Lf}+\frac{(V_i-V_o)(t-t_{i-1})}{L}\qquad t\in[t_{i-1},t_i] \tag{7}$$

where $i_L(t_0)$ is the only element implicit and can be calculable via the establishment of another parameter-relation existing in inductor current of MIbC topology — the averaged inductor current over the *i*th-subinterval (I_{Li}) and the averaged inductor current over one complete operating period (I_L). To integrate (7) from $d_{i-1}T$ to d_iT yields the GFE for I_{Li},

$$I_{Li}=i_L(t_0)d_i+\frac{d_i\sum_1^{i-1}(V_j-V_o)d_j}{Lf}+\frac{(V_i-V_o)d_i^2}{2Lf}\qquad t\in[t_{i-1},t_i] \tag{8}$$

The GFE for I_L is obtained simply by accumulating (8) from i = 1 to m+1,

$$I_L=i_L(t_0)+\frac{\sum_1^{m}\left[(V_i-V_o)d_i\sum_{i+1}^{m+1}d_j\right]}{Lf}+\frac{\sum_1^{m+1}(V_i-V_o)d_i^2}{2Lf} \tag{9}$$

to which the basic circuit relation, i.e., $I_L = V_o / R_o$, is applied to get the GFE of $i_L(t_0)$,

$$i_L(t_0)=\frac{V_o}{R_o}-\frac{\sum_1^{m}\left[(V_i-V_o)d_i\sum_{i+1}^{m+1}d_j\right]}{Lf}-\frac{\sum_1^{m+1}(V_i-V_o)d_i^2}{2Lf} \tag{10}$$

Equating (10) to zero allows boundary inductance of L between CCM and DCM,

$$L_b=\frac{R_o\left\{\sum_1^{m}\left[(V_i-V_o)d_i\sum_{i+1}^{m+1}d_j\right]-\sum_1^{m+1}(V_i-V_o)d_i^2/2\right\}}{V_of} \tag{11}$$

Substituting (10) back into (7) to (9) leads to final explicit GFEs for all common-inductor-current-related steady-state quantities.

B. DCM Scenario with TEM-based TSS Scheme

In CCM, the key point of the derivation is to establish the calculable GFE for $i_L(t_0)$; in DCM, as is shown in Fig. 3(b), waveform of i_L drops to zero by the end of one operating period, implying $i_L(t_0)$ = 0. But its termination time-point, or rather its nonzero-i_L freewheeling duration, $d_{m+1}T$, is unknown. An additional subinterval, $d_{m+2}T$, also known as the zero-i_L freewheeling period, should be employed, as well as the diverse duty-ratio relation $d_{m+1}+d_{m+2}=1-\sum_1^m d_i$. That means the steady-state analysis and computation in DCM must be distinguishing from those in CCM.

Equation set (1) can be directly inherited here with few modifications as follows,

$$i_L(t)=\begin{cases}(V_1-V_o)(t-t_0)/L & t\in[t_o,t_1]\\ i_L(t_1)+(V_2-V_o)(t-t_1)/L & t\in[t_1,t_2]\\ \quad\vdots & \quad\vdots\\ i_L(t_{m-1})+(V_m-V_o)(t-t_{m-1})/L & t\in[t_{m-1},t_m]\\ i_L(t_m)-V_o(t-t_m)/L & t\in[t_m,t_{m+1}]\\ i_L(t_{m+1})+0 & t\in[t_{m+1},t_{m+2}]\end{cases} \tag{12}$$

where the term $i_L(t_{m+1})$ actually equals to zero. Rewrite (12) in the form of time-dependent GFE,

$$i_L(t)=\begin{cases}\dfrac{\sum_1^{i-1}(V_j-V_o)d_j}{Lf}+\dfrac{(V_i-V_o)(t-t_{i-1})}{L} & t\in[t_{i-1},t_i]\\ 0 \quad t\in[t_{m+1},t_{m+2}]\end{cases} \tag{13}$$

where i = 1, 2, …, m+1. Similar to (3), the ith-subinterval inductor current ripple is generalized to

$$|\Delta i_{Li}|=\begin{cases}\dfrac{|V_i-V_o|d_i}{Lf} & t\in[t_{i-1},t_i]\\ 0 \quad t\in[t_{m+1},t_{m+2}]\end{cases} \tag{14}$$

followed by the GFE for $|\Delta i_L|$,

$$|\Delta i_L|=\frac{|V_i-V_o|\sum_1^m d_i}{Lf}\ \text{or}=\frac{V_o d_{m+1}}{Lf} \tag{15}$$

which coincides to (4). In accordance with the algebraic relation mentioned in (5), the input-to-output GFE for DCM is derived as

$$V_o=\sum_1^m V_i d_i/\sum_1^{m+1} d_i \tag{16}$$

However, it is not the explicit GFE for V_o since d_{m+1} is undetermined. Explicit GFE for d_{m+1} or V_o cannot be directly solved, while one of the alternatives is to solve a nonlinear equation in numerical way,

$$V_o^2\left(1-\sum_1^m d_i\right)=R_o T\left[\sum_1^m d_i(V_i-V_o)\right]^2/(2L) \tag{17}$$

Reference [17] presented the detail about its derivation, which was based upon the energy balance stored in C over the nonzero-i_L freewheeling period. After yielding the explicit GFE for V_o, deforming (16) can lead the GFE for d_{m+1},

$$d_{m+1}=\sum_1^m(V_i/V_o-1)d_i \tag{18}$$

With the help of (17) and (18) then, the GFEs for I_{Li} and I_L can be readily solved through (13),

$$I_{Li}=\begin{cases}\dfrac{d_i\sum_1^{i-1}(V_j-V_o)d_j}{Lf}+\dfrac{(V_i-V_o)d_i^2}{2Lf} & t\in[t_{i-1},t_i]\\ 0 \quad t\in[t_{m+1},t_{m+2}]\end{cases} \tag{19}$$

$$I_L = \frac{\sum_1^m \left[(V_i - V_o) d_i \sum_{i+1}^{m+1} d_j \right]}{Lf} + \frac{\sum_1^{m+1} (V_i - V_o) d_i^2}{2Lf} \tag{20}$$

Similarities in the derivation results between CCM and DCM allow the following synthesis for both scenarios (see Appendix-A).

C. CCM Scenario with IDEM-based TSS Scheme

If IDEM-based TSS scheme in Fig. 2(c) is applied, waveform of i_L should respond as Fig. 3(c). There are $2m$ subintervals ($\sum_1^{2m} d_i = 1$), including m freewheeling periods (i.e., d_2, d_4, …, d_{2m}). The inductor current profile has the piecewise expression as

$$i_L(t) = \begin{cases} i_L(t_0) + (V_1 - V_o)(t - t_0)/L & t \in [t_0, t_1] \\ i_L(t_1) - V_o (t - t_1)/L & t \in [t_1, t_2] \\ i_L(t_2) + (V_2 - V_o)(t - t_2)/L & t \in [t_2, t_3] \\ i_L(t_3) - V_o (t - t_3)/L & t \in [t_3, t_4] \\ \vdots & \vdots \\ i_L(t_{2m-2}) + (V_m - V_o)(t - t_{2m-2})/L & t \in [t_{2m-2}, t_{2m-1}] \\ i_L(t_{2m-1}) - V_o (t - t_{2m-1})/L & t \in [t_{2m-1}, t_{2m}] \end{cases} \tag{21}$$

Generalize (21) to

$$i_L(t) = i_L(t_{i-1}) + \frac{(V_{(i+1)/2} - V_o)(t - t_{i-1})}{L} \quad t \in [t_{i-1}, t_i] \tag{22}$$

where $i = 1, 2, \ldots, 2m$, and $V_{(i+1)/2}$ have values only if their subscripts are integers, otherwise equal to zero (i.e., $V_{0.5} = V_{1.5} = V_{2.5} = \ldots = V_{(2m+1)/2} = 0$). Inductor current ripples for subintervals are generalized to

$$|\Delta i_{Li}| = \frac{|V_{(i+1)/2} - V_o| d_i}{L} \quad t \in [t_{i-1}, t_i] \tag{23}$$

The GFE for $|\Delta i_L|$ is the discrepancy between the maximum of $\{i_L(t_1), i_L(t_3), \ldots, i_L(t_{2m-1})\}$ and the minimum of $\{i_L(t_2), i_L(t_4), \ldots, i_L(t_{2m})\}$, which can be expressed as

$$|\Delta i_L| = \max\{i_L(t_i), i = 1, 3, \cdots, 2m-1\} - \min\{i_L(t_i), i = 2, 4, \cdots, 2m\} \tag{24}$$

The fact that the net change in i_L over one T equals to zero enables (23) applicable for derivation of input-to-output GFE

$$V_o = \sum_1^{2m} V_{(i+1)/2} d_i \tag{25}$$

With the similar iteration process to TEM, the generalization of (22) can be performed as

$$i_L(t) = i_L(t_0) + \frac{\sum_1^{i-1} (V_{(j+1)/2} - V_o) d_j}{Lf} + \frac{(V_{(i+1)/2} - V_o)(t - t_{i-1})}{L} \quad t \in [t_{i-1}, t_i] \tag{26}$$

where only $i_L(t_0)$ remains implicit and calculable by repeating the geometric average algorithm applied to the TEM scenario. The GFE for I_{Li} and I_L are

$$I_{Li} = i_L(t_0)d_i + \frac{d_i\sum_1^{i-1}(V_{(j+1)/2} - V_o)d_j}{Lf} + \frac{(V_{(i+1)/2} - V_o)d_i^2}{2Lf} \qquad t \in [t_{i-1}, t_i] \tag{27}$$

$$I_L = i_L(t_0) + \frac{\sum_1^{2m-1}\left[(V_{(i+1)/2} - V_o)d_i\sum_{i+1}^{2m}d_j\right]}{Lf} + \frac{\sum_1^{2m}(V_{(i+1)/2} - V_o)d_i^2}{2Lf} \tag{28}$$

where $i_L(t_0)$ is implicit. Applying the basic circuit relation $I_L = V_o / R_o$ to (28) yields the explicit GFE for $i_L(t_0)$,

$$i_L(t_0) = \frac{V_o}{R_o} - \frac{\sum_1^{2m-1}\left[(V_{(i+1)/2} - V_o)d_i\sum_{i+1}^{2m}d_j\right]}{Lf} - \frac{\sum_1^{2m}(V_{(i+1)/2} - V_o)d_i^2}{2Lf} \tag{29}$$

Substituting (29) back into (26) to (28) leads to final explicit GFEs for all common-inductor-current-related steady-state quantities.

DCM scenario with IDEM-based TSS scheme is not involved here because of its specificity on operational condition.

Comment [#L10]: After cautious discussion, DCM scenario with IDEM-based TSS scheme is not going to be detailed here due to its impracticality and specificity on operational condition and parametric behavior. But the derivation details are given in the cover letter attached.

III. Synthesis and Other Issues

A. Generalization Procedures for MICs

Comment [#L11]: Generalization procedures are added here to provide an important reference to researchers when they are going to make analysis or design of other type of MIC topologies, such as MIbBC and MISEPIC. This synthesis made the proposed analytical methodology more general and complete, which is the most crucial part in this manuscript. Along with this, the corresponding flowchart is also designed for better understanding and utilization.

In the purpose of synthesis, procedures can be concluded from the derivation process in Section II in pursuit of explicit analytical expressions of any other MIC's topology:

Step 1: to observe the inductor current profile corresponding to the applied switching functions and determine the number of subintervals including (i.e., $n = f(m)$), followed by which the description equation set consisting of n time-dependent piecewise equations is established;

Step 2: to normalize the equation set in Step 1 to the time-dependent expression for i_L over the ith subinterval (i.e., $i_L(t)$, $t \in [t_{i-1}, t_i]$), according to which the inductor current ripple for each subinterval (i.e., $|\Delta i_{Li}|$) is available for generalization. Executing addition calculation to these GFEs for $|\Delta i_{Li}|$ in accordance with the appearance of i_L waveform leads to the GFE for the inductor current ripple over one T (i.e., $|\Delta i_L|$). If the extreme-value points of i_L are undetermined, "max" and "min" operators need to be employed to generalize $|\Delta i_L|$;

Step 3: the input-to-output GFE (i.e., $V_o = f(d_j)$, $i = 1, 2, \ldots, m$) is expressed by deforming the GFE for $|\Delta i_L|$ in Step 2. In CCM, duty ratios for all subintervals in one T are known quantities, thus explicit GFE for V_o is readily solved; in DCM, the freewheeling period splits into nonzero and zero subintervals with their corresponding duty ratios implicit, leaving V_o implicit;

Step 4: To apply iterative algorithm to the time-dependent GFE for i_L over the ith subinterval in Step 2 to obtaining the GFEs for $i_L(t)$ over the ith subinterval. In CCM, the GFEs for $i_L(t)$ should contain positive DC component, $i_L(t_0)$, which needs to be expressed explicitly; however in DCM, the GFEs for $i_L(t)$ are without $i_L(t_0)$ thus explicit;

Step 5: To calculate the explicit GFEs for V_o in DCM in Step 3 and $i_L(t_0)$ in CCM in Step 4. As for V_o in DCM, energy balance in capacitor is used to establish a nonlinear equation about V_o which only consists of known duty ratios and can be solved in numerical

way; as for $i_L(t_0)$ in CCM, the basic circuit relation $I_o = V_o / R_o$ is considered to make connection to the averaged inductor current, I_L, which can be solved by integrating $i_L(t)$ presented in Step 2 over T and dividing by T;

Step 6: To substitute the derivation results in Step 5 back into the relevant expressions appearing in Step 2-4 to yield all the explicit GFEs.

For better elucidation and utilization, the above generalization procedures are expressed in the flowchart Fig. 4, where the gray dashed lines represent the substitution operation in Step 6. Based upon such derivation procedures, topologies of MIbBC [2, 3, 17] and multiple-input single-ended primary-inductor converter (MISEPIC) [16, 19] given in Fig. 1(b) and (c), which have one sharing inductor in the circuits and of a wide range of applications, have been analyzed in their steady states. The GFEs for all concerned circuit's parameters are derived and enumerated in Appendix.

B. Issue on GFE Derivation for Output Capacitor Voltage

Comment [#L12]: Some other issues, such as GFEs for output capacitor voltage and power loss budgeting, are discussed in here. The former one is for the feasibility of the proposed method; the latter one for the better fitness between theoretical and tested results.

The above common inductor current GFEs are proposed on the assumption that V_o is invariable with respect to time. The time-dependent GFE for output capacitor voltage, $v_c(t)$, is theoretically derivable through equivalent generalization procedures to that in common inductor current, on the basis of the duality in circuit theory between inductance and capacitance. The exact steady-state analysis is challenged by the fact that the GFE derivation for $v_c(t)$ requires the detailed GFE for $i_L(t)$, rather than approximated averaged value I_L, in any subinterval involved. Take the simplest scenario that $m = 1$ in TEM-based MIbC circuit in CCM for instance,

$$v_c(t) = v_c(t_0) + \left[i_L(t_0)/C - v_c(t_0)/(R_oC)\right](t - t_0) \qquad t \in [t_0, t_1] \tag{30}$$

$$v_c(t_1) = v_c(t_0)\left[1 - d_1/(R_oCf)\right] + i_L(t_0)d_1/(Cf) \tag{31}$$

$$v_c(t) = \left[1 - \frac{d_1 - f + d_1/R_oC}{R_oCf}(t - t_1)\right]v_c(t_0) + \frac{(R_oC + t - t_1)d_1}{R_oC^2 f} i_L(t_0) + \frac{i_L(t_1)}{C}(t - t_1) \qquad t \in [t_1, t_2], \tag{32}$$

$$v_c(t_2) = \left[1 - \frac{d_1d_2 - fd_2 + d_1d_2/R_oC}{R_oCf}\right]v_c(t_0) + \frac{(R_oC + t - t_1)d_1}{R_oC^2 f} i_L(t_0) + \frac{i_L(t_1)d_2}{C} \tag{33}$$

$$v_c(t_0) = \frac{(R_oC + t - t_1)d_1 i_L(t_0) + R_oCfd_2 i_L(t_1)}{Cd_1d_2 - Cfd_2 + d_1d_2/R_o} \tag{34}$$

It proves the proposed generalization procedures are applicable for output capacitor voltage issue, but the complexity of the GFEs and the difficulty in derivation will sharply increase with the incremental of the number of inputs. For brevity, details would not be elaborated here.

C. Issue on Power Loss in GFEs

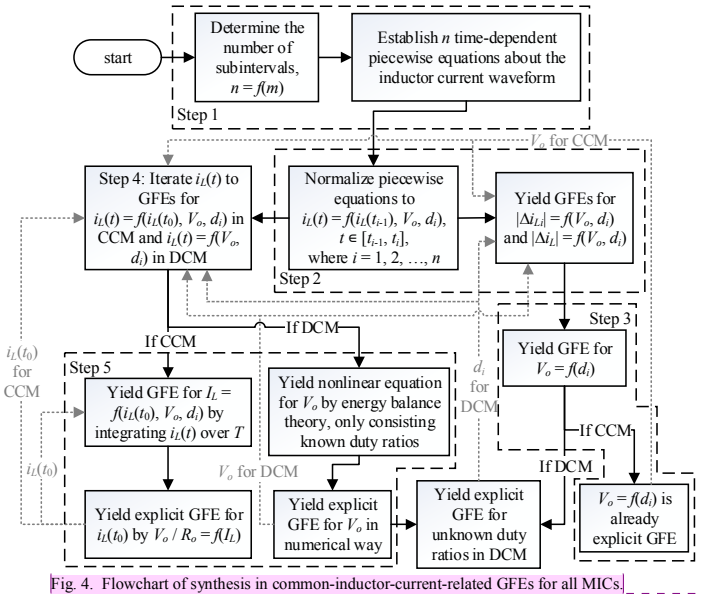

Fig. 4. Flowchart of synthesis in common-inductor-current-related GFEs for all MICs.

Comment [#L13]: Flowchart of the proposed synthesizing procedures is put forward here, where the black solid lines represent the derivation direction and gray dashed lines indicate substitution operation. The GFE for each parameter is explicit only when the substitution is complete.

In practice, parasitic elements of components applied in circuits would bring about considerable voltage drops and inductor current decrease. The parasitic elements of the MIC components, including ON-resistances, $R_{on,i}$, ON-state voltage drops, $V_{on,i}$, and the inductor resistance, R_L [3]. The modification is made on R_o and V_i for a nonideal MIC, expecting higher accuracy for experimental and practical purposes,

$$R_{o,loss} = R_o + R_L + \sum_1^n R_{on,i} d_i \tag{35}$$

$$V_{i,loss} = V_i - V_{on,i} d_i \tag{36}$$

IV. Case Study

A DIbC prototype was built for experimental verification of the previously proposed theory and equations. As is analyzed in Section II, there are 3 subintervals within one T in TEM-based CCM scenario, respectively accounting for d_1T, d_2T, and d_3T; one more subinterval, d_4T, which is actually a duration of i_L-nonzero freewheeling condition should be added after d_3T if the circuit is operating in TEM-based DCM; as for IDEM-based CCM scenario, d_1T and d_3T are switching-on subintervals while d_2T and d_4T are freewheeling subintervals.

A. Hardware Installation

Power MOSFETs (model: IRFP4110PbF) were chosen as the switches and a 84.5μH-power-inductor (model: WCM-323-18) as L. Detailed parameters are listed in Table II, and the entire experimental platform is shown in Fig. 5.

TABLE II CIRCUIT PARAMETERS FOR EXPERIMENTS

Symbol	VALUE	Symbol	VALUE	SYMBOL	VALUE
V_1	20-25 V	V_2	10-15 V	$V_{on,i}$	1.6 V
L	84.5 μH	C	470 μF	R_o	3.7-5.3 Ω
$R_{on,i}$	3.7 mΩ	R_L	20 mΩ	f	5-25 kHz

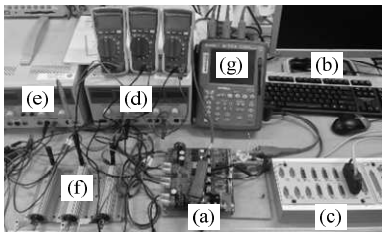

Fig. 5. Hardware installation: (a) DIbC, (b) host computer, (c) dSPACE CP1103 controller board, (d) input source V_1, (e) input source V_2, (f) output load: fixed power resistors, and (g) oscilloscope.

B. Comparison Results and Discussion in TEM-Based Scenario

Nine groups of experiments with different converter's parameters settings were conducted, where Test 1 was set as the reference test and the following 8 tests were set up by modifying one parameter in the reference test at a time. The oscilloscope's screenshots of the dynamics of i_L and switching functions are provided at the left side of Fig. 6, while the theoretical calculation results were plotted at the right side of Fig. 6 accordingly for comparison. Due to page limitation, only the circuit waveforms of the reference test in CCM and DCM are given in Fig. 6, for the data collected in Table III be completely reflective of the theoretical and experimental results. Data of V_o, I_L, I_{L1}, I_{L2}, $i_L(t_0)$, $i_L(t_1)$, $i_L(t_2)$, and d_4T were multiple-sampled and averaged in Table III, as well as the GFE-calculated results. Relative error, ε, of all the 8 test objectives between theoretical and test values were given at last. Minor relative error (< 1%) appears high accuracy of the GFEs.

Some conclusions benefiting to MICs' behavior analysis and circuit design can be drawn from the comparison results:

(a) Compared with Test 1 and Test 4, the values of V_o and I_L were subject to V_i and d_i, but not affected by voltage arrangement order.

(b) Reducing f to DCM level (e.g., Test 9) pulled V_o up while pushing I_L down.

(c) Compared with Test 1 and Test 2, the value of I_{L2} was positively correlated to its previous-conducted source voltage V_1 (I_{L2} = 0.616 A when V_1 = 20 V; I_{L2} = 0.745 A when V_1 = 25 V).

(d) Comparison between Test 1 and Test 3 proved increasing voltage of V_i enhances I_{Li}.

(e) The values of I_{Li} increased when the conduction sequence of V_i is moved behind. For example, 20V-source was conducting ahead of 10V-source in Test 1 and served as V_1, then I_{L1} = 0.368 A; while in Test 4, 20V-source turned to V_2 which was conducting behind 10V-source, then I_{L2} = 0.524 A.

(f) Higher than that in Test 1, the value of d_1 in Test 5 not only increased I_{L1} (I_{L1} = 0.368 A when d_1 = 0.25; I_{L1} = 0.527 A when d_1 = 0.3), but also enhanced I_{L2} (I_{L2} = 0.616 A when d_1 = 0.25; I_{L2} = 0.693 A when d_1 = 0.3). So did d_2.

(g) Although turning f up can increase the DC component $i_L(t_0)$, it was clear in the comparison between Test 1 and Test 7 that changes on I_{L1} and I_{L2} were polarized. I_{L1} increases (from 0.368 A to 0.384 A) while I_{L2} reduced (from 0.616 A to 0.582 A).

(h) The result that lighter load (or higher R_o) pulled every current-related value down from Test 1 to Test 8 was beyond reproach.

Comment [#L14]: The following 9 conclusions drawn from the experiments are benefiting to the MIC's operation behavior analysis and circuit design. The choice of modulation type, arrangement of input voltages, and boundaries of duty ratios and frequency in the circuit design can be determined more reasonably. We only present the conclusions that we found in the experiments of this study, and according to these conclusions researchers can benefit from variety of issues in the circuit design. However, due to page limitation and less correlation to the research scope of this manuscript, we are unable to discuss them one by one, just briefly mentioning in here and the Conclusion part.

TABLE III DATA COLLECTION FROM EXPERIMENTS AND CALCULATIONS FOR 9 TESTS ON TEM-BASED DIBC WITH DIFFERENT PARAMETERS SETTINGS

No.	Setting	GFE/Test	V_o (V)	I_L (A)	I_{L1} (A)	I_{L2} (A)	$i_L(t_0)$ (A)	$i_L(t_1)$ (A)	$i_L(t_2)$ (A)	d_4T (μs)	ε (%)
1	Reference test[a]	GFE	6.700	1.800	0.372	0.620	0.624	2.355	2.606	0	0.984
		Test	6.633	1.782	0.368	0.616	0.603	2.338	2.590	0	N/A
2	V_1: 20→25 V	GFE	7.950	2.136	0.456	0.750	0.683	2.968	3.035	0	0.995
		Test	7.869	2.114	0.451	0.745	0.658	2.950	3.015	0	N/A
3	V_2: 10→15 V	GFE	7.950	2.136	0.410	0.704	0.868	2.413	3.220	0	0.948
		Test	7.874	2.116	0.405	0.700	0.843	2.394	3.202	0	N/A
4	V_1: 20→10 V V_2: 10→20 V	GFE	6.700	1.800	0.280	0.528	0.994	1.245	2.976	0	0.965
		Test	6.635	1.783	0.275	0.524	0.973	1.229	2.961	0	N/A
5	d_1: 0.25→0.3	GFE	7.620	2.047	0.530	0.696	0.811	2.725	2.840	0	0.969
		Test	7.573	2.035	0.527	0.693	0.788	2.707	2.821	0	N/A
6	d_2: 0.25→0.3	GFE	7.120	1.913	0.394	0.758	0.743	2.412	2.639	0	0.963
		Test	7.051	1.894	0.390	0.752	0.722	2.394	2.622	0	N/A
7	f: 20→25 kHz	GFE	6.700	1.800	0.388	0.586	0.859	2.244	2.445	0	0.942
		Test	6.634	1.783	0.384	0.582	0.840	2.227	2.428	0	N/A
8	R_o: 3.7→5.3 Ω	GFE	6.700	1.259	0.237	0.485	0.083	1.814	2.065	0	0.732
		Test	6.650	1.250	0.235	0.483	0.070	1.806	2.058	0	N/A
9	f: 20→5 kHz (CCM→DCM)	GFE	8.273	2.691	0.635	1.364	0	4.403	4.459	38.020	1.103
		Test	8.111	2.442	0.565	1.141	0	4.509	4.622	38.120	N/A

[a]Parameters setting in the reference test is: $V_1 = 20$ V, $V_2 = 10$ V, $d_1 = 0.25$, $d_2 = 0.25$, f=20 kHz, and $R_o = 3.7$ Ω. The others are identical to Test 1 except the parameter modification given in its corresponding blank of the table.
[b]N/A: not applicable.

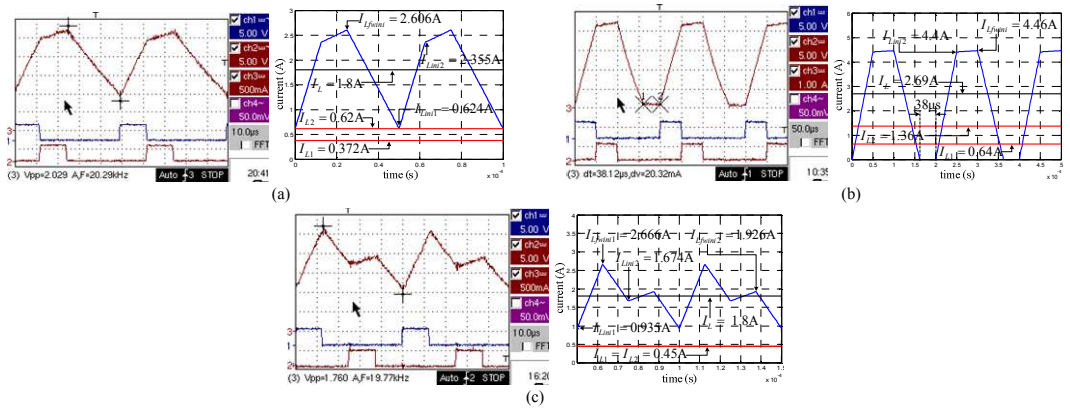

Fig. 6. Circuit waveforms obtained from experimental measurements (left) and UM calculations (right) of common inductor current of TEM-based DIbC with the setting: (a) $V_1 = 20$ V, $d_1 = 0.25$, $V_2 = 10$ V, $d_2 = 0.25$, $R_o = 3.7$ Ω, f = 20 kHz, (b) identical to (a) except f = 8 kHz (at DCM), and (c) IDEM-based DIbC with identical setting to (a) except $d_1 = d_2 = d_3 = d_4 = 0.25$.

(i) Theoretical and testing results showed that value-increases in d_4, I_L, I_{L1}, I_{L2}, $i_L(t_1)$, and $i_L(t_2)$ attributed to the rise of V_o.

C. *Comparison Results and Discussion in IDEM-Based Scenario*

Similarly, we conducted 8 groups of experiments with the same settings as Test 1 to Test 8 in the TEM tests (d_2 and d_4 equal to 0.225 in Test 5 and Test 6, while equal to 0.25 in the other 6 tests). The Test 9 was afterwards carried out, where the duty ratios of the two freewheeling subintervals were set unequal (i.e., $d_2 = 0.3$ and $d_4 = 0.2$). Ideal matching results were obtained ($\varepsilon \le 0.6\%$) for the first 8 tests. The similarities between TEM and IDEM cases on the dynamics of the test objectives under different parameters settings for the first 8 tests are obvious, when referring to Table III and Table IV; thus, the analysis of these discussion are skipped for brevity. It should be noted that $i_L(t_0)$ in test 4 was no longer the minimum value of i_L over one T, because V_1 and V_2 were inter-

Comment [#L15]: Experimental tables are improved, cancelling data that is less relevant to the topic of this manuscript.

TABLE IV DATA COLLECTION FROM EXPERIMENTS AND CALCULATIONS FOR 9 TESTS ON IDEM-BASED DIBC WITH DIFFERENT PARAMETERS SETTINGS

No.	Setting	GFE/Test	V_o (V)	I_L (A)	I_{L1} (A)	I_{L2} (A)	I_{Lim1} (A)	I_{Lfwin1} (A)	I_{Lim2} (A)	I_{Lfwin2} (A)	ε (%)
1	reference test[a]	GFE	6.700	1.800	0.450	0.450	0.935	2.666	1.674	1.926	0.564
		Test	6.662	1.790	0.448	0.447	0.923	2.657	1.665	1.915	N/A
2	V_1: 20→25 V	GFE	7.950	2.136	0.534	0.534	0.993	3.279	2.103	2.169	0.549
		Test	7.904	2.124	0.531	0.531	0.980	3.269	2.091	2.156	N/A
3	V_2: 10→15 V	GFE	7.950	2.136	0.534	0.534	1.363	2.909	1.733	2.539	0.571
		Test	7.904	2.124	0.531	0.531	1.350	2.900	1.720	2.527	N/A
4	V_1: 20→10 V V_2: 10→20 V	GFE	6.700	1.800	0.450	0.450	1.674	1.926	0.935	2.666	0.566
		Test	6.662	1.790	0.448	0.448	1.664	1.915	0.923	2.657	N/A
5	d_1: 0.25→0.3	GFE	7.620	2.047	0.611	0.509	1.079	2.993	1.978	2.094	0.496
		Test	7.577	2.036	0.611	0.509	1.077	2.995	1.978	2.092	N/A
6	d_3: 0.25→0.3	GFE	7.120	1.913	0.472	0.566	1.052	2.720	1.772	2.000	0.640
		Test	7.079	1.902	0.476	0.571	1.066	2.738	1.789	2.015	N/A
7	f: 20→25 kHz	GFE	6.700	1.800	0.450	0.450	1.108	2.493	1.700	1.900	0.489
		Test	6.662	1.790	0.448	0.447	1.097	2.483	1.689	1.890	N/A
8	R_o: 3.7→5.3 Ω	GFE	6.700	1.259	0.315	0.315	0.394	2.124	1.133	1.385	0.402
		Test	6.673	1.254	0.314	0.314	0.387	2.121	1.128	1.379	N/A
9	d_2: 0.25→0.3 d_4: 0.25→0.2	GFE	6.700	1.800	0.471	0.422	1.020	2.751	1.562	1.813	0.896
		Test	6.662	1.790	0.463	0.413	0.986	2.720	1.528	1.779	N/A

[a]Parameters setting in the reference test is: V_1 = 20 V, V_2 = 10 V, $d_1 = d_2 = d_3 = d_4$ = 0.25, f=20 kHz, and R_o = 3.7 Ω. The others are identical to Test 1 except the parameter modification given in its corresponding blank of the table.

changed, which broke the voltage-descending order. The minimum value moved to $i_L(t_3)$ while the maximum value belonged to $i_L(t_4)$, making $|\Delta i_L| = i_L(t_4) - i_L(t_3)$. It verifies the correctness of (24).

V. CONCLUSION

An exact steady-state analysis tool to describing the operating behaviors of all the crucial circuit's parameters in MIC is proposed. GFEs for both TEM-based and IDEM-based MIbC are explicitly derived and expressed with the circuit's known quantities. The accuracy and feasibility are experimentally verified. The dynamics of the circuit's parameters under different TSS schemes show obvious disparities. Conclusions that are benefiting to MICs' behavior analysis and circuit design are drawn from the comparison results in the case study of a DIbC prototype. Common-inductor-current-related parameters, i.e., I_{Li}, I_L, $i_L(t)$, $i_L(t_i)$, $|\Delta i_{Li}|$, and $|\Delta i_L|$, are proven vulnerable to modulation type, conduction sequence, input-voltage, load value, duty ratio, and switching frequency. All these influences are precisely reflected in the proposed GFEs. The generalization procedures summarized in Section III can be referred to exact steady-state analysis in all MIC topologies.

Comment [#L16]: Words on benefits from this methodology to circuit analysis and design are added here.

APPENDIX

Comment [#L17]: Appendix is added to conclude GFEs for MIbBC and MISEPIC topologies in both TEM and IDEM scenarios, making the structure of the contents more integrated and complete, even for the convenience of readers' checking.

A. GFEs for MIbC in both CCM and DCM Scenarios with TEM-based Scheme

$$\begin{cases} V_o = \sum_1^m V_i d_i \Big/ \sum_1^{m+1} d_i \\ V_o^2\left(1-\sum_1^m d_i\right) = R_o T\left[\sum_1^m d_i (V_i - V_o)\right]^2 / (2L) \quad \text{(DCM only)} \end{cases} \tag{A.1}$$

$$d_{m+1} = \sum_1^m (V_i / V_o - 1) d_i \tag{A.2}$$

$$d_{m+2} = 1 - \sum_1^{m+1} d_i \quad \text{(DCM only)} \tag{A.3}$$

$$i_L(t)=\begin{cases} i_L(t_0)+\dfrac{\sum_1^{i-1}\left(V_j-V_o\right)d_j}{Lf}+\dfrac{(V_i-V_o)(t-t_{i-1})}{L} & t\in\left[t_{i-1},t_i\right] \\ 0 \quad t\in\left[t_{m+1},t_{m+2}\right] \quad \text{(DCM only)} \end{cases} \tag{A.4}$$

$$\left|\Delta i_{Li}\right|=\begin{cases} \dfrac{\left|V_i-V_o\right|d_i}{Lf} & t\in\left[t_{i-1},t_i\right] \\ 0 \quad t\in\left[t_{m+1},t_{m+2}\right] \quad \text{(DCM only)} \end{cases} \tag{A.5}$$

$$\left|\Delta i_L\right|=\frac{\left|V_i-V_o\right|\sum_1^m d_i}{Lf} \text{ or } =\frac{V_o d_{m+1}}{Lf} \tag{A.6}$$

$$I_{Li}=\begin{cases} i_L(t_0)d_i+\dfrac{d_i\sum_1^{i-1}\left(V_j-V_o\right)d_j}{Lf}+\dfrac{(V_i-V_o)d_i^2}{2Lf} & t\in\left[t_{i-1},t_i\right] \\ 0 \quad t\in\left[t_{m+1},t_{m+2}\right] \quad \text{(DCM only)} \end{cases} \tag{A.7}$$

$$I_L=i_L(t_0)+\frac{\sum_1^m\left[(V_i-V_o)d_i\sum_{i+1}^{m+1}d_j\right]}{Lf}+\frac{\sum_1^{m+1}(V_i-V_o)d_i^2}{2Lf} \tag{A.8}$$

$$i_L(t_0)=\begin{cases} \dfrac{V_o}{R_o}-\dfrac{\sum_1^m\left[(V_i-V_o)d_i\sum_{i+1}^{m+1}d_j\right]}{Lf}-\dfrac{\sum_1^{m+1}(V_i-V_o)d_i^2}{2Lf} & \text{(CCM only)} \\ 0 \quad \text{(DCM only)} \end{cases} \tag{A.9}$$

$$L_b=\frac{R_o\left\{\sum_1^m\left[(V_i-V_o)d_i\sum_{i+1}^{m+1}d_j\right]-\sum_1^{m+1}(V_i-V_o)d_i^2/2\right\}}{V_o f} \tag{A.10}$$

where $i = 1, 2, \ldots, m+1$ and $V_{m+1} = 0$.

B. GFEs for MIbBC in both CCM and DCM Scenarios with TEM-based Scheme

$$V_o=\begin{cases} \sum_1^m V_i d_i / d_{m+1} \\ \sqrt{R_o/(2Lf)}\cdot\sum_1^m V_i d_i \quad \text{(DCM only) [17]} \end{cases} \tag{A.11}$$

$$d_{m+1}=\sum_1^m V_i d_i / V_o \tag{A.12}$$

$$d_{m+2}=1-\sum_1^{m+1}d_i \quad \text{(DCM only)} \tag{A.13}$$

$$i_L(t)=\begin{cases} i_L(t_0)+\dfrac{\sum_1^{i-1}V_j d_j}{Lf}+\dfrac{V_i(t-t_{i-1})}{L} & t\in\left[t_{i-1},t_i\right] \\ 0 \quad t\in\left[t_{m+1},t_{m+2}\right] \quad \text{(DCM only)} \end{cases} \tag{A.14}$$

$$\left|\Delta i_{Li}\right|=\begin{cases} \dfrac{\left|V_i\right|d_i}{Lf} & t\in\left[t_{i-1},t_i\right] \\ 0 \quad t\in\left[t_{m+1},t_{m+2}\right] \quad \text{(DCM only)} \end{cases} \tag{A.15}$$

$$\left|\Delta i_L\right|=\frac{\left|V_i\right|\sum_1^m d_i}{Lf} \text{ or } =\frac{V_o d_{m+1}}{Lf} \tag{A.16}$$

$$I_{Li}=\begin{cases} i_L(t_0)d_i+\dfrac{d_i\sum_1^{i-1}V_j d_j}{Lf}+\dfrac{V_i d_i^2}{2Lf} & t\in\left[t_{i-1},t_i\right] \\ 0 \quad t\in\left[t_{m+1},t_{m+2}\right] \quad \text{(DCM only)} \end{cases} \tag{A.17}$$

$$I_L = i_L(t_0) + \frac{\sum_1^m \left(V_i d_i \sum_{i+1}^{m+1} d_j \right)}{Lf} + \frac{\sum_1^{m+1} V_i d_i^2}{2Lf} \tag{A.18}$$

$$i_L(t_0) = \begin{cases} \dfrac{V_o}{R_o(1-\sum_1^m d_i)} - \dfrac{\sum_1^m \left(V_i d_i \sum_{i+1}^{m+1} d_j \right)}{Lf} - \dfrac{\sum_1^{m+1} V_i d_i^2}{2Lf} & \text{(CCM only)} \\ 0 \quad \text{(DCM only)} \end{cases} \tag{A.19}$$

$$L_b = \frac{R_o(1-\sum_1^m d_i)\left[\sum_1^m \left(V_i d_i \sum_{i+1}^{m+1} d_j \right) + \sum_1^{m+1} V_i d_i^2 / 2 \right]}{V_o f} \tag{A.20}$$

where $i = 1, 2, \ldots, m+1$ and $V_{m+1} = -V_o$.

C. GFEs for MIbBC in CCM Scenario with IDEM-based Scheme

$$V_o = \sum_1^m V_i d_{2i-1} / \sum_1^m d_{2i} \tag{A.21}$$

$$\sum_1^{2m} d_i = 1 \tag{A.22}$$

$$i_L(t) = i_L(t_0) + \frac{\sum_1^{i-1} V_{(j+1)/2} d_j}{Lf} + \frac{V_{(i+1)/2}(t - t_{i-1})}{L} \qquad t \in [t_{i-1}, t_i] \tag{A.23}$$

$$\left| \Delta i_{Li} \right| = \frac{\left| V_{(i+1)/2} \right| d_i}{Lf} \qquad t \in [t_{i-1}, t_i] \tag{A.24}$$

$$\left| \Delta i_L \right| = \max \left\{ i_L(t_i), i = 1, 3, \cdots, 2m-1 \right\} - \min \left\{ i_L(t_i), i = 2, 4, \cdots, 2m \right\} \tag{A.25}$$

$$I_{Li} = i_L(t_0) d_i + \frac{d_i \sum_1^{i-1} V_{(j+1)/2} d_j}{Lf} + \frac{V_{(i+1)/2} d_i^2}{2Lf} \qquad t \in [t_{i-1}, t_i] \tag{A.26}$$

$$I_L = i_L(t_0) + \frac{\sum_1^{2m-1} \left(V_{(i+1)/2} d_i \sum_{i+1}^{2m} d_j \right)}{Lf} + \frac{\sum_1^{2m} V_{(i+1)/2} d_i^2}{2Lf} \tag{A.27}$$

$$i_L(t_0) = \frac{V_o}{R_o(1-\sum_1^m d_i)} - \frac{\sum_1^{2m-1} \left(V_{(i+1)/2} d_i \sum_{i+1}^{2m} d_j \right)}{Lf} - \frac{\sum_1^{2m} V_{(i+1)/2} d_i^2}{2Lf} \tag{A.28}$$

where $i = 1, 2, \ldots, 2m$ and $V_{0.5} = V_{1.5} = V_{2.5} = \ldots = V_{(2m+1)/2} = -V_o$.

D. GFEs for MISEPIC in both CCM and DCM Scenarios with TEM-based Scheme

$$V_o = \begin{cases} \sum_1^m V_i d_i / d_{m+1} \\ \sqrt{\dfrac{R}{2f}\left[\left(\sum_1^m V_i d_i \right)^2 / L + \sum_1^m \left(\sum_1^m V_j d_j \right)^2 / L_i - 2f^2 \sum_1^m E_{ci} \right]} \quad \text{(DCM only) [17]} \end{cases} \tag{A.29}$$

$$d_{m+1} = \sum_1^m V_i d_i / V_o \tag{A.30}$$

$$d_{m+2} = 1 - \sum_1^{m+1} d_i \quad \text{(DCM only)} \tag{A.31}$$

$$\begin{cases} \begin{cases} i_{Lk}(t) = i_{Lk}(t_0) + \dfrac{\sum_1^{i-1} V_j d_j}{L_k f} + \dfrac{V_i (t - t_{i-1})}{L_k} \\ i_L(t) = i_L(t_0) + \dfrac{\sum_1^{i-1} V_j d_j}{Lf} + \dfrac{V_i (t - t_{i-1})}{L} \end{cases} & t \in [t_{i-1}, t_i] \\ \begin{cases} i_{Lk}(t) = 0 \\ i_L(t) = 0 \end{cases} & t \in [t_{m+1}, t_{m+2}] \end{cases} \tag{A.32}$$

$$\begin{cases} \begin{cases} |\Delta i_{Lki}| = \dfrac{|V_i| d_i}{L_k f} \\ |\Delta i_{Li}| = \dfrac{|V_i| d_i}{Lf} \end{cases} & t \in [t_{i-1}, t_i] \\ \begin{cases} |\Delta i_{Lki}| = 0 \\ |\Delta i_{Li}| = 0 \end{cases} & t \in [t_{m+1}, t_{m+2}] \quad \text{(DCM only)} \end{cases} \tag{A.33}$$

$$\begin{cases} |\Delta i_{Lk}| = \dfrac{|V_i| \sum_1^m d_i}{L_k f} \text{ or } = \dfrac{V_o d_{m+1}}{L_k f} \\ |\Delta i_L| = \dfrac{|V_i| \sum_1^m d_i}{Lf} \text{ or } = \dfrac{V_o d_{m+1}}{Lf} \end{cases} \tag{A.34}$$

$$\begin{cases} I_{Lk} = i_{Lk}(t_0) + \dfrac{\sum_1^m \left(V_i d_i \sum_{i+1}^{m+1} d_j \right)}{L_k f} + \dfrac{\sum_1^{m+1} V_i d_i^2}{2 L_k f} \\ I_L = i_L(t_0) + \dfrac{\sum_1^m \left(V_i d_i \sum_{i+1}^{m+1} d_j \right)}{Lf} + \dfrac{\sum_1^{m+1} V_i d_i^2}{2Lf} \end{cases} \tag{A.35}$$

$$\begin{cases} \begin{cases} i_{Lk}(t_0) = \dfrac{V_o d_k}{R_o (1 - \sum_1^m d_i)} - \dfrac{\sum_1^m \left(V_i d_i \sum_{i+1}^{m+1} d_j \right)}{Lf} - \dfrac{\sum_1^{m+1} V_i d_i^2}{2Lf} \\ i_L(t_0) = \dfrac{V_o}{R_o} - \dfrac{\sum_1^m \left(V_i d_i \sum_{i+1}^{m+1} d_j \right)}{Lf} - \dfrac{\sum_1^{m+1} V_i d_i^2}{2Lf} \end{cases} & \text{(CCM only)} \\ \begin{cases} i_{Lk}(t_0) = 0 \\ i_L(t_0) = 0 \end{cases} & \text{(DCM only)} \end{cases} \tag{A.36}$$

$$\begin{cases} L_{kb} = \dfrac{R_o (1 - \sum_1^m d_i) \left[\sum_1^m \left(V_i d_i \sum_{i+1}^{m+1} d_j \right) + \sum_1^{m+1} V_i d_i^2 / 2 \right]}{V_o d_k f} \\ L_b = \dfrac{R_o \left[\sum_1^m \left(V_i d_i \sum_{i+1}^{m+1} d_j \right) + \sum_1^{m+1} V_i d_i^2 / 2 \right]}{V_o f} \end{cases} \tag{A.37}$$

where $i = 1, 2, \ldots, m+1$, $k = 1, 2, \ldots, m$, $V_{m+1} = -V_o$. The subscript "*Lki*" represents the input inductor L_k operating in the ith subinterval. The symbol E_{ci} denotes the energy stored in C_k during $d_{m+1}T$ can be solved through

$$E_{ci} = \frac{d_{m+1} d_i V_i I_{Lei} \left[2C_i (1 - d_i) f V_i + \left(2 \sum_{i+1}^m d_j + d_i + d_{m+1} - 1 \right) I_{Lei} d_i \right]}{2C_i (1 - d_i)^2 f^2} \tag{A.38}$$

where I_{Lei} is equivalent to the sum of the averaged inductor currents except I_{Li}, i.e.,

$$I_{Lei} = \sum_1^{i-1} I_{Lj} + \sum_{i+1}^m I_{Lj} + I_L \tag{A.39}$$

E. GFEs for MISEPIC in CCM Scenario with IDEM-based Scheme

$$V_o = \sum_1^m V_i d_{2i-1} / \sum_1^m d_{2i} \tag{A.40}$$

$$\sum_1^{2m} d_i = 1 \tag{A.41}$$

$$\begin{cases} i_{Lk}(t) = i_{Lk}(t_0) + \dfrac{\sum_1^{i-1} V_{(j+1)/2} d_j}{L_k f} + \dfrac{V_{(i+1)/2}(t - t_{i-1})}{L_k} \\ i_L(t) = i_L(t_0) + \dfrac{\sum_1^{i-1} V_{(j+1)/2} d_j}{Lf} + \dfrac{V_{(i+1)/2}(t - t_{i-1})}{L} \end{cases} \quad t \in [t_{i-1}, t_i] \tag{A.42}$$

$$\begin{cases} \left|\Delta i_{Lki}\right| = \dfrac{\left|V_{(i+1)/2}\right| d_i}{L_k f} \\ \left|\Delta i_{Li}\right| = \dfrac{\left|V_{(i+1)/2}\right| d_i}{Lf} \end{cases} \quad t \in [t_{i-1}, t_i] \tag{A.43}$$

$$\begin{cases} \left|\Delta i_{Lk}\right| = \max\left\{i_{Lk}(t_i), i = 1,3,\cdots,2m-1\right\} - \min\left\{i_{Lk}(t_i), i = 2,4,\cdots,2m\right\} \\ \left|\Delta i_L\right| = \max\left\{i_L(t_i), i = 1,3,\cdots,2m-1\right\} - \min\left\{i_L(t_i), i = 2,4,\cdots,2m\right\} \end{cases} \tag{A.44}$$

$$\begin{cases} I_{Lk} = i_{Lk}(t_0) + \dfrac{\sum_1^{2m-1}\left[V_{(i+1)/2} d_i \sum_{i+1}^{2m} d_j\right]}{L_k f} + \dfrac{\sum_1^{2m} V_{(i+1)/2} d_i^2}{2L_k f} \\ I_L = i_L(t_0) + \dfrac{\sum_1^{2m-1}\left[V_{(i+1)/2} d_i \sum_{i+1}^{2m} d_j\right]}{Lf} + \dfrac{\sum_1^{2m} V_{(i+1)/2} d_i^2}{2Lf} \end{cases} \tag{A.45}$$

$$\begin{cases} i_{Lk}(t_0) = \dfrac{V_o}{R_o(1 - \sum_1^m d_i)} - \dfrac{\sum_1^{2m-1}\left(V_{(i+1)/2} d_i \sum_{i+1}^{2m} d_j\right)}{L_k f} - \dfrac{\sum_1^{2m} V_{(i+1)/2} d_i^2}{2L_k f} \\ i_L(t_0) = \dfrac{V_o}{R_o} - \dfrac{\sum_1^{2m-1}\left(V_{(i+1)/2} d_i \sum_{i+1}^{2m} d_j\right)}{Lf} - \dfrac{\sum_1^{2m} V_{(i+1)/2} d_i^2}{2Lf} \end{cases} \tag{A.46}$$

where $i = 1, 2, \ldots, 2m$, $k = 1, 2, \ldots, m$, and $V_{0.5} = V_{1.5} = V_{2.5} = \ldots = V_{(2m+1)/2} = -V_o$.

REFERENCE

[1] L. Xian, G. Wang, and Y. Wang, "Circuitry and analysis of input-capacitor-added multiple-input buck converters," *Power Electronics, IET,* vol. 6, pp. 1415-1426, 2013.

[2] C. N. Onwuchekwa and A. Kwasinski, "A Modified-Time-Sharing Switching Technique for Multiple-Input DC-DC Converters," *Power Electronics, IEEE Transactions on,* vol. 27, pp. 4492-4502, 2012.

[3] H. Behjati and A. Davoudi, "A Multiple-Input Multiple-Output DC-DC Converter," *Industry Applications, IEEE Transactions on,* vol. 49, pp. 1464-1479, 2013.

[4] R. Ahmadi, H. Zargarzadeh, and M. Ferdowsi, "Nonlinear Power Sharing Controller for a Double-Input H-Bridge-Based Buckboost-Buckboost Converter," *Power Electronics, IEEE Transactions on,* vol. 28, pp. 2402-2414, 2013.

[5] Y. Dongsheng, Y. Min, and R. Xinbo, "One-Cycle Control for a Double-Input DC/DC Converter," *Power Electronics, IEEE Transactions on,* vol. 27, pp. 4646-4655, 2012.

[6] H. F. Wu, K. Sun, S. Ding, and Y. Xing, "Topology Derivation of Nonisolated Three-Port DC-DC Converters From DIC and DOC," *Ieee Transactions on Power Electronics,* vol. 28, pp. 3297-3307, Jul 2013.

[7] F. Liu, Z. Wang, Y. Mao, and X. Ruan, "Asymmetrical Half-Bridge Double-Input DC/DC Converters Adopting Pulsating Voltage Source Cells for Low Power Applications," *Power Electronics, IEEE Transactions on,* vol. PP, pp. 1-1, 2013.

[8] L. Xian, G. Wang, and Y. Wang, "Implementation and control of a double-input DC/DC converter for PEMFC/battery hybrid power supply," in *Industrial Electronics and Applications (ICIEA), 2012 7th IEEE Conference on*, 2012, pp. 285-290.

[9] X. Liang and W. Youyi, "Current-limited voltage control strategies for multiple-input buck converters applied in renewable energy hybrid systems," in *IPEC, 2012 Conference on Power & Energy*, 2012, pp. 434-438.

[10] Q. Zhijun, O. Abdel-Rahman, H. Al-Atrash, and I. Batarseh, "Modeling and Control of Three-Port DC/DC Converter Interface for Satellite Applications," *Power Electronics, IEEE Transactions on,* vol. 25, pp. 637-649, 2010.

[11] Y. Li, D. S. Yang, and X. B. Ruan, "Interleaved Dual-Edge Modulation Scheme for Double-Input Converter to Minimize Inductor Current Ripple," *2008 Ieee Power Electronics Specialists Conference, Vols 1-10,* pp. 1783-1789, 2008.

[12] D. Somayajula and M. Ferdowsi, "Power Sharing in a Double-Input Buckboost Converter Using Offset Time Control," in *Applied Power Electronics Conference and Exposition, 2009. APEC 2009. Twenty-Fourth Annual IEEE*, 2009, pp. 1091-1096.

[13] K. Sudareswaran, B. Hariprasad, P. Sankar, P. S. R. Nayak, and S. Sankar, "A voltage constrained time sharing switching scheme for dual input buck converter," in *Power Electronics, Drives and Energy Systems (PEDES), 2012 IEEE International Conference on*, 2012, pp. 1-5.

[14] W. Rong-Jong, L. Chung-You, L. Jun-Jie, and C. Yung-Ruei, "Newly Designed ZVS Multi-Input Converter," *Industrial Electronics, IEEE Transactions on,* vol. 58, pp. 555-566, 2011.

[15] S. Chao, B. Miller, K. Mayaram, and T. Fiez, "A Multiple-Input Boost Converter for Low-Power Energy Harvesting," *Circuits and Systems II: Express Briefs, IEEE Transactions on,* vol. 58, pp. 827-831, 2011.

[16] Z. Ruichen, Y. Sheng-Yang, and A. Kwasinski, "Modeling of multiple-input DC-DC converters considering input-coupling effects," in *Energy Conversion Congress and Exposition (ECCE), 2011 IEEE*, 2011, pp. 698-705.

[17] A. Khaligh, J. Cao, and Y. J. Lee, "A Multiple-Input DC-DC Converter Topology," *Ieee Transactions on Power Electronics,* vol. 24, pp. 862-868, Mar-Apr 2009.

[18] L. Yan, R. Xinbo, Y. Dongsheng, and L. Fuxin, "Modeling, analysis and design for hybrid power systems with dual-input DC/DC converter," in *Energy Conversion Congress and Exposition, 2009. ECCE 2009. IEEE*, 2009, pp. 3203-3210.

[19] Z. Ruichen and A. Kwasinski, "Analysis of decentralized controller for multiple-input converters," in *Applied Power Electronics Conference and Exposition (APEC), 2012 Twenty-Seventh Annual IEEE*, 2012, pp. 1853-1860.